

## Optimal joint estimation of multiple Rabi frequencies

Hongzhen Chen and Haidong Yuan\*

*Department of Mechanical and Automation Engineering, The Chinese University of Hong Kong, Shatin, Hong Kong*



(Received 1 October 2018; published 26 March 2019)

We study the joint estimation of multiple Rabi frequencies in a multilevel system. By analytically identifying the optimal probe state and the optimal measurement, we obtain the highest precision limit for the joint estimation of multiple Rabi frequencies. We show that the joint estimation does not always outperform the separate estimation. In different regimes the joint estimation can either outperform or underperform the separate estimation. We further show that if additional adaptive quantum controls are allowed then the advantage of the joint estimation over the separate estimation can be reestablished.

DOI: 10.1103/PhysRevA.99.032122

### I. INTRODUCTION

Quantum metrology, which makes use of quantum mechanical effects to achieve higher precision [1,2], is gaining increasing attention for its broad applications in atomic clocks [3–7], spectroscopy [8–11], magnetometry [12–15], gravitational-wave detection [16–19], etc. Much progress has been made in the single-parameter quantum estimation [1,2,20–22]. However, in many practical applications such as microscopy and imaging [23–29], there is typically more than one parameter. This creates a high demand for better understanding of multiparameter quantum estimation. There have been recent studies on joint estimation of multiple parameters in various specific settings, such as multiple phase estimation under commuting dynamics [30], estimation of multidimensional fields [31], estimation of multiple parameters in quantum states [32,33] and unitary operators [34–40], joint estimation of the phase and decoherence rate [41,42], and joint estimation of two decoherence rates [43]. However, the optimal performance for multiparameter quantum estimation is still not well understood [44–46]. While general methods on the identification of the optimal probe states exist for the single-parameter quantum estimation [47–49], the probe states for multiparameter quantum estimation are typically chosen heuristically [31,36,43]. The optimal probe states are only identified for very few cases in multiparameter quantum estimation [30,42,50].

In this article, we study the joint estimation of multiple Rabi frequencies. We start with the joint estimation of two Rabi frequencies in a three-level system. By explicitly optimizing the probe state and the measurement, we analytically obtain the highest precision for the joint estimation of two Rabi frequencies. We find that, in contrast to the expectation, the joint estimation does not always outperform the separate estimation. There exist different regimes in which the joint estimation can either outperform or underperform the separate estimation. This enriches the understandings on the relationship between the joint estimation and the separate estimation.

We then consider adding optimal quantum controls in the scheme and show that with the adaptive quantum controls the joint estimation can restore the advantage over the separate estimation.

The article is organized as follows. In Sec. II we make a brief introduction of the basic tools for the multiparameter quantum estimation. In Sec. III we derive the precision limits for the joint estimation of two Rabi frequencies in a three-level system by explicitly obtaining the optimal probe state and the optimal measurement; we then compare the joint estimation with the separate estimation in Sec. IV. In Sec. V we show that with optimal adaptive controls the joint estimation can always outperform the separate estimation. This is then generalized to systems with more levels in Sec. VI. Section VII concludes the paper.

### II. MULTIPARAMETER QUANTUM ESTIMATION

To estimate a set of parameters,  $\varphi = (\varphi_1, \dots, \varphi_p)$ , encoded in a quantum channel,  $\Lambda_\varphi$ , one can prepare a probe state,  $\rho$ , and get the output state  $\rho_\varphi = \Lambda_\varphi(\rho)$ , which contains the unknown parameters. With a set of positive-operator-valued measurements,  $\{M_x\}_{x \in \Omega}$ , the information of the parameters can then be extracted. From the probability distribution of the measurement results,  $p_\varphi(x) = \text{Tr}(\rho_\varphi M_x)$ , one can construct an estimator,  $\hat{\varphi}(x) = (\hat{\varphi}_1, \dots, \hat{\varphi}_p)(x)$ . For a locally unbiased estimator with  $\langle \hat{\varphi} \rangle = \sum_{x \in \Omega} \hat{\varphi}(x) p_\varphi(x) = \varphi$  and  $d\langle \hat{\varphi} \rangle / d\varphi_i = 1$ ,  $\forall i$ , the precision is bounded below by the Fisher information matrix [51–54] as

$$\text{Cov}(\hat{\varphi}) \geq \mathcal{I}(\varphi)^{-1}, \quad (1)$$

where  $\text{Cov}(\hat{\varphi})$  is the covariance matrix with its  $ij$ th entry given as  $[\text{Cov}(\hat{\varphi})]_{ij} = \langle (\hat{\varphi}_i - \varphi_i)(\hat{\varphi}_j - \varphi_j) \rangle$ , and  $\mathcal{I}(\varphi)$  is the Fisher information matrix with its  $ij$ th entry given by [51,54]

$$[\mathcal{I}(\varphi)]_{ij} = \sum_{x \in \Omega} \frac{\partial \ln p_\varphi(x)}{\partial \varphi_i} \frac{\partial \ln p_\varphi(x)}{\partial \varphi_j} p_\varphi(x). \quad (2)$$

The Fisher information matrix can be further bounded by the quantum Fisher information matrix (QFIM), which leads

\*hdyuan@mae.cuhk.edu.hk

to the quantum Cramér-Rao bound (QCRB) [55–57] as

$$\langle \hat{\phi} \rangle \geqslant \mathcal{I}(\phi)^{-1} \geqslant J(\phi)^{-1}. \quad (3)$$

Here the  $ij$ th entry of the QFIM is given by

$$[J(\phi)]_{ij} = \frac{1}{2} \text{Tr}(\rho_\phi \{L_i, L_j\}), \quad (4)$$

where  $\{\bullet, \bullet\}$  is the anticommutator and  $L_i$  is the symmetrical logarithm derivative (SLD) of the  $i$ th parameter, which can be obtained by  $\partial_\phi \rho_\phi = (L_i \rho_\phi + \rho_\phi L_i)/2$ . If the weaker commutation conditions,

$$\text{Tr}(\rho_\phi [L_i, L_j]) = 0, \quad \forall i, j, \quad (5)$$

are satisfied, the quantum Cramer-Rao bound can be saturated [45,58–60]. However, in general the quantum Cramer-Rao bound is not achievable. In that case, a weight matrix,  $W$ , is often added in the figure of merit as  $\text{Tr}[W \text{Cov}(\hat{\phi})]$ , one can then identify the optimal probe state and the optimal measurement according to the figure of merit. In this article, we take  $W = I$  and consider the figure of merit as  $\text{Tr}[\text{Cov}(\hat{\phi})]$ . From the QCRB, it is easy to get a lower bound as

$$\text{Tr}[\text{Cov}(\hat{\phi})] \geqslant \text{Tr}[J(\phi)^{-1}]. \quad (6)$$

### III. MULTIPARAMETER ESTIMATION IN A THREE-LEVEL SYSTEM

We first consider a three-level system interacting with two resonating fields with the  $\Lambda$ - or ladder-shape linkage, as depicted in Fig. 1. The dynamics of the system is described by the Schrödinger equation

$$i\hbar \frac{d}{dt} |\psi\rangle = H(\Omega)|\psi\rangle, \quad (7)$$

where  $H(\Omega)$  is the Hamiltonian of the system, which, under the rotating-wave approximation, can be written as

$$H(\Omega) = \frac{1}{2} \begin{pmatrix} 0 & \Omega_1 & 0 \\ \Omega_1 & 0 & \Omega_2 \\ 0 & \Omega_2 & 0 \end{pmatrix}. \quad (8)$$

Here  $\Omega_1$  and  $\Omega_2$  are two Rabi frequencies which we would like to estimate.

If we take the initial state as  $|\psi_{\text{in}}\rangle$ , then the output state is given by  $|\psi_\Omega\rangle = U(\Omega, t)|\psi_{\text{in}}\rangle$ , where  $U(\Omega, t) = e^{-iH(\Omega)t}$ . The SLD operators with respect to  $\Omega_1$  and  $\Omega_2$  can be computed as

$$L_i = 2(|\partial_i \psi_\Omega\rangle \langle \psi_\Omega| + |\psi_\Omega\rangle \langle \partial_i \psi_\Omega|), \quad (9)$$

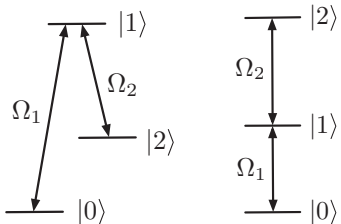


FIG. 1. Three-level systems with  $\Lambda$ - or ladder-shape linkage.

where  $\partial_i$  denotes the partial derivative with respect to the  $i$ th parameter  $\Omega_i$ ,  $|\partial_i \psi_\Omega\rangle = \frac{\partial U(\Omega, t)}{\partial \Omega_i} |\psi_{\text{in}}\rangle$ . The quantum Fisher information matrix is then given by

$$\begin{aligned} [J_\Omega]_{ij} &= \frac{1}{2} \text{Tr}(|\psi_\Omega\rangle \langle \psi_\Omega| \{L_i, L_j\}) \\ &= 2(\langle \partial_i \psi_\Omega | \partial_j \psi_\Omega \rangle + \langle \partial_j \psi_\Omega | \partial_i \psi_\Omega \rangle) + 4 \langle \partial_i \psi_\Omega | \psi_\Omega \rangle \\ &\quad \times \langle \partial_j \psi_\Omega | \psi_\Omega \rangle, \end{aligned} \quad (10)$$

where  $[J_\Omega]_{ij}$  is the  $ij$ th entry of the quantum Fisher information matrix. For pure states, the weaker conditions in Eq. (5) take the form of  $\text{Im}(\langle \partial_i \psi_\Omega | \partial_j \psi_\Omega \rangle) = 0, \forall i, j$  [45,58].

To optimize the figure of merit, we need to identify the optimal probe state and the optimal measurement. We first identify the optimal probe state that has the minimal value of  $\text{Tr}[J(\phi)^{-1}]$ ; then we show the quantum Cramer-Rao bound given in Eq. (6) can be saturated, ensuring the optimal figure of merit. To ease the calculation, we use the eigenvectors of the Hamiltonian as a basis. The eigenbasis, denoted as  $|\Phi_0\rangle$  and  $|\Phi_\pm\rangle$ , and the corresponding eigenvalues, denoted as  $\Omega_0$  and  $\Omega_\pm$ , of  $H(\Omega)$  are as follows:

$$\begin{aligned} \Omega_0: |\Phi_0\rangle &= \cos \vartheta |0\rangle - \sin \vartheta |2\rangle, \\ \Omega_+: |\Phi_+\rangle &= \frac{1}{\sqrt{2}} (\sin \vartheta |0\rangle + |1\rangle + \cos \vartheta |2\rangle), \\ \Omega_-: |\Phi_-\rangle &= \frac{1}{\sqrt{2}} (\sin \vartheta |0\rangle - |1\rangle + \cos \vartheta |2\rangle), \end{aligned} \quad (11)$$

where  $\Omega_0 = 0$ ,  $\Omega_\pm = \pm \frac{1}{2} \sqrt{\Omega_1^2 + \Omega_2^2}$ , and  $\vartheta$  is the mixing angle with  $\tan \vartheta = \Omega_1/\Omega_2$ .

These eigenbases form a complete basis for the Hilbert space, we can thus write the initial probe state as  $|\psi_{\text{in}}\rangle = C_0 |\Phi_0\rangle + C_+ |\Phi_+\rangle + C_- |\Phi_-\rangle$ , where  $C_0 \in \mathbb{R}$  and  $C_\pm \in \mathbb{C}$  are coefficients to be optimized. Note that this is just a way to write the initial probe state in terms of the eigenbasis; the initial probe state is fixed once it is chosen. The output state can now be easily obtained as

$$\begin{aligned} |\psi_\Omega\rangle &= e^{-iH(\Omega)t} |\psi_{\text{in}}\rangle = \left( \sum_{n=0,\pm} e^{-i\Omega_n t} |\Phi_n\rangle \langle \Phi_n| \right) |\psi_{\text{in}}\rangle \\ &= \sum_{n=0,\pm} C_n e^{-i\Omega_n t} |\Phi_n\rangle. \end{aligned} \quad (12)$$

The partial derivative of the output state can be obtained as

$$\begin{aligned} |\partial_i \psi_\Omega\rangle &= \left( \sum_{n=0,\pm} \partial (e^{-i\Omega_n t} |\Phi_n\rangle \langle \Phi_n|) / \partial \Omega_i \right) |\psi_{\text{in}}\rangle \\ &= \sum_{n=0,\pm} [((\partial_i \Phi_n) |\psi_{\text{in}}\rangle - it C_n \partial_i \Omega_n) e^{-i\Omega_n t} |\Phi_n\rangle \\ &\quad + C_n e^{-i\Omega_n t} |\partial_i \Phi_n\rangle]. \end{aligned} \quad (13)$$

This can then be substituted into Eq. (10) to get the quantum Fisher information matrix (see the Appendix for detailed calculations). The quantum Fisher information matrix turns out to have different behaviors at different time points. There exist some specific time points at which the quantum Fisher information matrix is singular while at other time points the quantum Fisher information matrix is full rank.

Specifically at the time points where  $\Omega_+t = 2n\pi$  for  $n \in \mathbb{N}$ , the quantum Fisher information matrix is singular, and it takes the following form:

$$J_\Omega = 4t^2[1 - C_0^2 - (|C_+|^2 - |C_-|^2)^2] \\ \times \begin{pmatrix} (\partial_1\Omega_+)^2 & (\partial_1\Omega_+)(\partial_2\Omega_+) \\ (\partial_2\Omega_+)(\partial_1\Omega_+) & (\partial_2\Omega_+)^2 \end{pmatrix}. \quad (14)$$

Intuitively, at these time point,  $U(\Omega, t) = e^{-iH(\Omega)t} = I$ , the dynamics is always the identity operator as long as  $\frac{1}{2}\sqrt{\Omega_1^2 + \Omega_2^2}t = 2n\pi$ . One cannot tell the differences between different pairs of  $\Omega_1$  and  $\Omega_2$  as long as they have the same norm. This indicates that at these time points the joint estimation of  $\Omega_1$  and  $\Omega_2$  is not possible.

---


$$\text{Tr}(J_\Omega^{-1}) = \frac{[(\partial_1\vartheta)(\partial_1\vartheta) + (\partial_2\vartheta)(\partial_2\vartheta)]A + 2[(\partial_1\vartheta)(\partial_1\Omega_+) + (\partial_2\vartheta)(\partial_2\Omega_+)]C + [(\partial_1\Omega_+)(\partial_1\Omega_+) + (\partial_2\Omega_+)(\partial_2\Omega_+)]B}{[(\partial_1\vartheta)(\partial_2\Omega_+) - (\partial_2\vartheta)(\partial_1\Omega_+)]^2(AB - C^2)} \\ = \frac{(1/4\Omega_+^2)A + (1/4)B}{(1/16\Omega_+^2)(AB - C^2)} = \frac{4A}{AB - C^2} + \frac{4\Omega_+^2B}{AB - C^2}. \quad (16)$$


---

In the Appendix, we show that the minimal value of  $\text{Tr}(J_\Omega^{-1})$  is achieved when the initial probe state is  $|\phi_{\text{in}}\rangle = \frac{P^*}{\sqrt{2|P|}}|\Phi_+\rangle + \frac{P}{\sqrt{2|P|}}|\Phi_-\rangle$ , and the corresponding minimal value of  $\text{Tr}(J_\Omega^{-1})$  is

$$\min \text{Tr}(J_\Omega^{-1}) = \frac{1}{t^2} + \frac{\Omega_+^2}{4\sin^2(\Omega_+t/2)}. \quad (17)$$

It can be checked directly that the weaker commutative conditions,  $\text{Im}(\partial_i\psi_\Omega|\partial_j\psi_\Omega) = 0, \forall i, j$ , hold in this case, and thus this minimal value can be saturated by some proper measurements. For example, one set of the measurements that saturate the quantum Cramer-Rao bound is  $\Pi_1 = |\gamma_1\rangle\langle\gamma_1|$ ,  $\Pi_2 = |\gamma_2\rangle\langle\gamma_2|$ ,  $\Pi_3 = |\gamma_3\rangle\langle\gamma_3|$ , and  $\Pi_4 = I - \Pi_1 - \Pi_2 - \Pi_3$ , where

$$|\gamma_1\rangle = |\psi_\Omega\rangle, \quad |\gamma_2\rangle = \frac{|\partial_1\psi_\Omega\rangle}{\sqrt{\langle\partial_1\psi_\Omega|\partial_1\psi_\Omega\rangle}}, \\ |\gamma_3\rangle = \frac{\langle\partial_2\psi_\Omega|\gamma_2\rangle|\gamma_2\rangle - \langle\partial_2\psi_\Omega\rangle}{\sqrt{\langle\partial_2\psi_\Omega|\partial_2\psi_\Omega\rangle} - \langle\partial_2\psi_\Omega|\gamma_2\rangle^2}. \quad (18)$$

#### IV. COMPARISON BETWEEN THE JOINT ESTIMATION AND THE SEPARATE ESTIMATION

We compare the performances of the joint estimation and the separate estimation. The separate estimation is to estimate  $\Omega_1$  and  $\Omega_2$  separately. For each round of experiments, one can use the dynamical decoupling to remove one of the fields and reduce the problem to the single-parameter estimation. For example, by applying periodic  $\pi$  pulses along the direction  $(|0\rangle\langle 1| + |1\rangle\langle 0|)/2$ , one can remove  $\Omega_2$  in the Hamiltonian and obtain the effective Hamiltonian  $H_1 = \Omega_1(|0\rangle\langle 1| + |1\rangle\langle 0|)/2$ . The quantum Fisher information (QFI) for the single parameter is

$$J[\rho(t)] = 4t^2[\text{Tr}(\rho_{\text{in}}H_1^2) - [\text{Tr}(\rho_{\text{in}}H_1)^2]], \quad (19)$$

At other time points, the entries of the quantum Fisher information matrix are given by (see the Appendix for detailed calculations)

$$[J_\Omega]_{ij} = 2((\partial_i\psi_\Omega|\partial_j\psi_\Omega) + (\partial_j\psi_\Omega|\partial_i\psi_\Omega)) + 4(\partial_i\psi_\Omega|\psi_\Omega) \\ \times (\partial_j\psi_\Omega|\psi_\Omega) \\ = (\partial_i\vartheta)(\partial_j\vartheta)A + (\partial_i\Omega_+)(\partial_j\Omega_+)B + [(\partial_i\vartheta)(\partial_j\Omega_+) \\ + (\partial_j\vartheta)(\partial_i\Omega_+)]C, \quad (15)$$

where  $A = -8C_0^2\text{Im}^2M + 4C_0^2|P|^2 + 2|M|^2$ ,  $B = -4t^2\frac{\text{Re}^2(MN^*)}{|P|^4} + 4t^2 - 4C_0^2t^2$ , and  $C = -4\sqrt{2}C_0\text{Im}M\frac{\text{Re}(MN^*)}{|P|^2}t + 2\sqrt{2}C_0t\text{Im}N$ , with  $P = e^{-i\Omega_+t} - 1$ ,  $M = C_+^*P^* + C_-^*P$ , and  $N = C_+^*P^* - C_-^*P$ . It is straightforward to obtain

where  $\rho_{\text{in}}$  is the initial probe state. The optimal probe state that maximizes the quantum Fisher information is [21,22]

$$|\psi_{\text{in}}\rangle = \frac{1}{\sqrt{2}}(|\lambda_{\text{min}}\rangle + |\lambda_{\text{max}}\rangle), \quad (20)$$

where  $\lambda_{\text{min}}$  and  $\lambda_{\text{max}}$  are the minimal and maximal eigenvalues of  $H_1$  with  $|\lambda_{\text{min}}\rangle$  and  $|\lambda_{\text{max}}\rangle$  denoting the corresponding eigenstates. For  $H_1 = (|0\rangle\langle 1| + |1\rangle\langle 0|)/2$ , the maximal QFI is  $J = t^2$ . Similarly, the maximal QFI for the separate estimation of  $\Omega_2$  is also  $J = t^2$ .

For comparison, we assume that the experiments are repeated  $m$  times for the estimation of each parameter in the separate estimation. For the joint estimation, the experiments are repeated  $2m$  times so the total number of experiments are the same. The quantum Cramér-Rao bound for the joint estimation is given by

$$\text{Tr}[\text{Cov}(\hat{\Omega})] \geqslant \frac{1}{2m}\text{Tr}(J_\Omega^{-1}) = \frac{1}{2mt^2} + \frac{\Omega_+^2}{8m\sin^2(\Omega_+t/2)}. \quad (21)$$

For the separate estimation, the minimal variance given by the quantum Cramér-Rao bound is  $\text{Var}(\hat{\Omega}_i) \geqslant \frac{1}{mt^2}, i \in \{1, 2\}$ . The total variance is

$$\text{Tr}[\text{Cov}(\hat{\Omega})] = \text{Var}(\hat{\Omega}_1) + \text{Var}(\hat{\Omega}_2) \geqslant \frac{2}{mt^2}. \quad (22)$$

The comparison of the performances is shown in Fig. 2; it can be seen that in the short time regime the joint estimation outperforms the separate estimation, while in the long time regime the joint estimation underperforms the separate estimation.

#### V. ESTIMATION WITH THE ADAPTIVE CONTROL

So far we have considered the highest precision achievable by optimizing the probe state and the measurement,

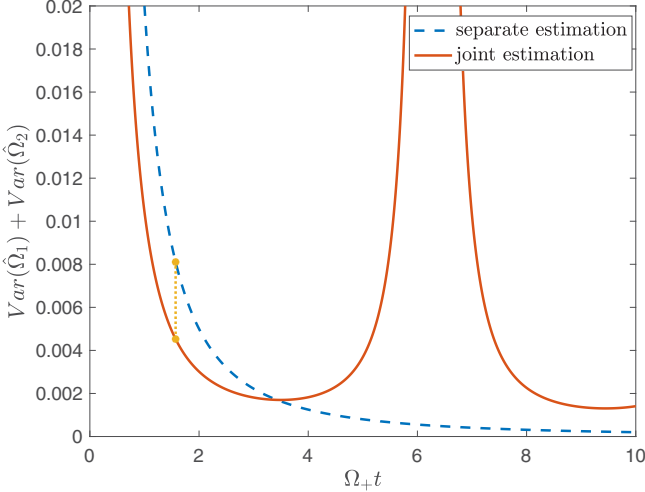


FIG. 2. Comparison of the joint estimation (solid line) of multiple frequencies with the separate estimation (dashed line), where the  $x$  axis is  $\Omega_+ t$  and the  $y$  axis is the total variance  $Var(\hat{\Omega}_1) + Var(\hat{\Omega}_2)$ . (Without loss of generality, here we set  $\Omega_+ = 0.1$  and  $m = 1$ .) The dotted vertical line shows the difference between these two schemes at the point of  $\Omega_+ t = \pi/2$ .

assuming the dynamics is fixed as  $U(\Omega, t) = e^{-iH(\Omega)t}$ . In practice, however, additional controls can often be added during the evolutions. As depicted in Fig. 3, the total evolution time  $t$  can be divided into  $N$  intervals with  $dt = t/N$ , and adaptive controls,  $U_1, U_2, \dots, U_N$ , can be added [50,61–64]. For such a control-enhanced sequential scheme, it has been shown that for any unitary evolution,  $U(\Omega, t) = e^{-iH(\Omega)t}$ , the optimal controls take the form of  $U_1 = U_2 = \dots = U_N = U^\dagger(\Omega, dt)$ , where  $\Omega$  is the true value of the parameter [50,61]. In practice, the true value is not known *a priori*; so the controls can only be taken as  $U_1 = U_2 = \dots = U_N = U^\dagger(\hat{\Omega}, dt)$ , with  $\hat{\Omega}$  being the estimated value, and need to be updated adaptively when more data are collected. When the estimated value is close to the true value, the total evolution is

$$\begin{aligned} (U_1 U_{dt})^N &= (e^{iH(\hat{\Omega})dt} e^{-iH(\Omega)dt})^N \\ &\approx \{(I + iH(\hat{\Omega})dt)[I - iH(\Omega)dt]\}^N \\ &\approx \{I - i[H(\Omega - \hat{\Omega})]dt\}^N \\ &\approx e^{-iH(\Omega - \hat{\Omega})t}. \end{aligned} \quad (23)$$

The effective Hamiltonian of the total dynamics is therefore  $H(\Omega - \hat{\Omega})$ . It can be seen from Fig. 4 that the total variance is quite robust against the estimation error. Asym-

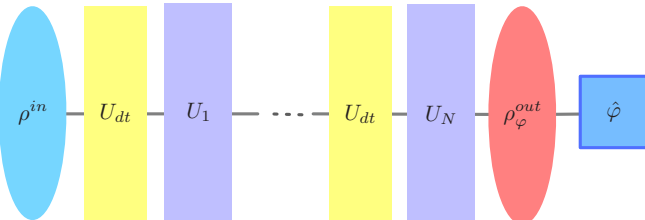


FIG. 3. Sequential unitary control.

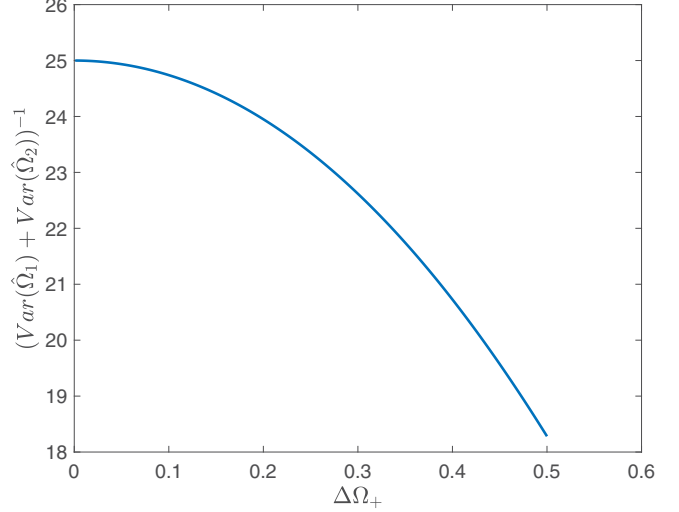


FIG. 4. The variation of the total variance at time  $t = 5$  with respect to the estimation error. Here the  $x$  axis is the estimation error,  $\Delta\Omega_+ \equiv \sqrt{(\Omega_1 - \hat{\Omega}_1)^2 + (\Omega_2 - \hat{\Omega}_2)^2}$ , and  $y$  axis is the inverse of the total variance,  $[Var(\hat{\Omega}_1) + Var(\hat{\Omega}_2)]^{-1}$ . It shows that the total variance is quite robust against the estimation error; it changes quite slowly with the estimation error.

totically, when the estimation converges to the true value, i.e., when  $\hat{\Omega} = \Omega$ , the adaptive control converges to the optimal control and the problem reduces to the joint estimation of  $\Omega = (\Omega_1, \Omega_2)$  at the point (0,0). At this point the optimal probe state is  $|\psi_{opt}\rangle = |1\rangle$ , and the total variance can be obtained by taking  $\Omega_+ \rightarrow 0$  in Eq. (21), which gives

$$\text{Tr}[\text{Cov}(\hat{\Omega})] = \frac{1}{mt^2}. \quad (24)$$

This always has a twofold improvement over the separate estimation. By taking the limit  $(\Omega_1, \Omega_2) \rightarrow (0, 0)$  in Eq. (18), one can verify that one set of the optimal measurements that saturate the QCRB is  $\mathcal{M} \equiv \{|0\rangle\langle 0|, |1\rangle\langle 1|, |2\rangle\langle 2|\}$ .

When  $\Delta\Omega \equiv (\Delta\Omega_1, \Delta\Omega_2) = (\Omega_1 - \hat{\Omega}_1, \Omega_2 - \hat{\Omega}_2)$  are not zero, the dynamics has the effective Hamiltonian  $H(\Delta\Omega)$ , and the total variance can be obtained from Eq. (21) as

$$\begin{aligned} \text{Tr}[\text{Cov}(\hat{\Omega})] &= \frac{1}{2mt^2} + \frac{\Delta\Omega_1^2 + \Delta\Omega_2^2}{8m \sin^2(\sqrt{\Delta\Omega_1^2 + \Delta\Omega_2^2}t/2)} \\ &= \frac{1}{mt^2} + \frac{\Delta\Omega_1^2 + \Delta\Omega_2^2}{24m} + O(\Delta\Omega^4). \end{aligned} \quad (25)$$

To see how quickly  $\hat{\Omega}$  approaches its true value under the adaptive control, we perform a numerical simulation of the adaptive procedure as follows.

(i) Choose an initial estimation of  $(\Omega_1, \Omega_2)$ , either randomly or from some prior knowledge, as  $(\hat{\Omega}_1^{(0)}, \hat{\Omega}_2^{(0)})$ , and construct the control,  $U^\dagger(\hat{\Omega}^{(0)}, dt)$ , with this estimated value.

(ii) Choose the initial probe state as  $|1\rangle$ , let the system evolve for a period of time  $t$ , and then perform the projective

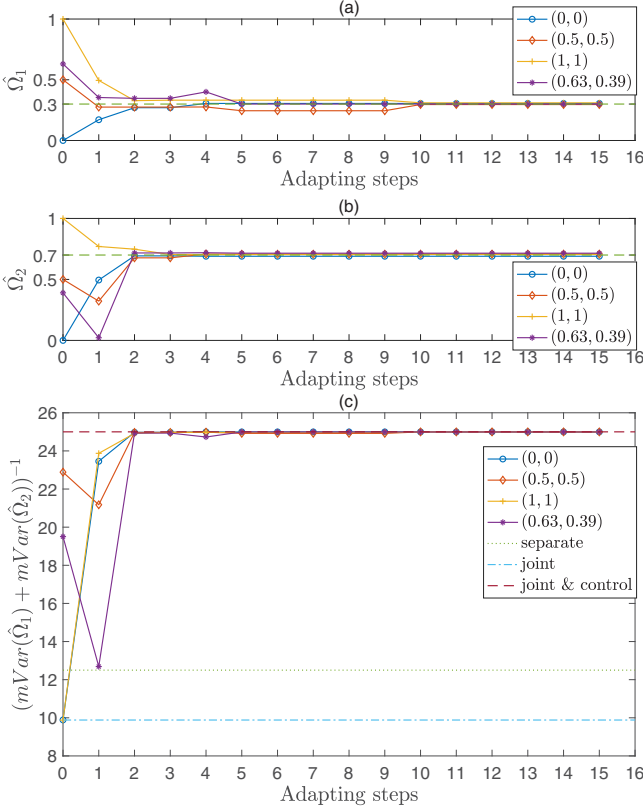


FIG. 5. Precision of the estimations at time  $t = 5$  after different adaptive steps. The true values of the parameters are  $\Omega_1 = 0.3$  and  $\Omega_2 = 0.7$ . The  $x$  axis is the adapting steps. For panels (a) and (b), the  $y$  axes are values of the estimators  $\hat{\Omega}_1$  and  $\hat{\Omega}_2$ , respectively. The  $y$  axis of panel (c) is the normalized total variance, i.e.,  $[m\text{Var}(\hat{\Omega}_1) + m\text{Var}(\hat{\Omega}_2)]^{-1}$ , where  $m = 30n$ , with  $n$  as the adapting steps. The dotted, dash-dotted, and dashed lines in panel (c) represent the total variance for the optimal separate estimation, the optimal joint estimation without control, and the optimal joint estimation with control, respectively. The four solid lines correspond to four different adaptive trajectories with four different initial guesses of the parameters,  $(\hat{\Omega}_1, \hat{\Omega}_2) = (0, 0), (0.5, 0.5), (1, 1)$ , and  $(0.63, 0.39)$ , respectively.

measurement,  $\mathcal{M} = \{|0\rangle\langle 0|, |1\rangle\langle 1|, |2\rangle\langle 2|\}$ , on the final state. Repeat this step for  $k = 30$  times.

(iii) Based on all the collected measurement results, use the maximum likelihood estimator to update the estimation of  $(\Omega_1, \Omega_2)$  to  $(\hat{\Omega}_1^{(1)}, \hat{\Omega}_2^{(1)})$ , and then update the control based on the new estimation.

(iv) Repeat Steps (i) and (iii).

The probe state and the measurement we choose in Step (ii) is the optimal probe state and the optimal measurement under the optimally controlled scheme. When the estimator approaches the true value, the adaptive scheme converges to the optimal scheme. It can be seen from Figs. 5(a) and 5(b) that, after just a few iterations, the estimators are already close to the true values. Figure 5(c) shows that, after just a couple of iterations, the controlled scheme already outperforms the uncontrolled schemes, and after a few iterations the precision under the adaptively controlled scheme is already close to the highest precision.

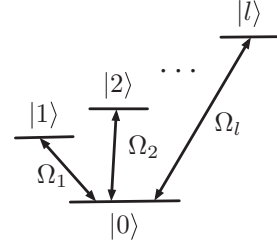


FIG. 6.  $l + 1$  energy levels with linkages from one level to the other  $l$  levels.

## VI. EXTENSION TO MULTIPLE LEVELS

The advantage of the joint estimation with adaptive controls can be extended to systems with more levels. We consider the system with  $l + 1$  levels, shown in Fig. 6, and estimate  $l$  Rabi frequencies between the ground state and the other  $l$  energy eigenstates. In this case the Hamiltonian is  $H_l(\Omega) = \sum_{i=1}^l \Omega_i E_i$ , where  $E_i = (|0\rangle\langle i| + |i\rangle\langle 0|)/2$ . The Rabi frequencies  $(\Omega_1, \Omega_2, \dots, \Omega_l)$  are the parameters to be estimated. For separate estimation, the quantum Fisher information for each parameter is  $J = t^2$ . If the experiment is repeated  $m$  times for each parameter, the total variance becomes

$$\sum_{i=1}^l \text{Var}(\hat{\Omega}_i) \geqslant \sum_{i=1}^l \frac{1}{mt^2} = \frac{l}{mt^2}. \quad (26)$$

For the joint estimation, by using the optimal adaptive control,  $U_1 = U_2 = \dots = U_N = e^{iH_l(\hat{\Omega})dt}$ , as described in Fig. 3 and choosing the initial state as  $|\psi_{\text{in}}\rangle = |0\rangle$ , we can obtain the quantum Fisher information matrix as  $[J_\Omega]_{ij} = t^2 \delta_{ij}$ . In this case, the weaker commutative condition also holds, and thus the quantum Cramer-Rao bound can be saturated. For comparison with the separate estimation, suppose the experiment is repeated for the same total number of times, which is  $lm$ , then the total variance for the joint estimation is

$$\sum_{i=1}^l \text{Var}(\hat{\Omega}_i) = \text{Tr}[\text{Cov}(\hat{\Omega})] \geqslant \frac{1}{lm} \text{Tr}(J^{-1}) = \frac{1}{mt^2}. \quad (27)$$

This has an  $l$ -fold improvement over the separate estimation. Intuitively, it can be understood that, for the estimation of each parameter  $\Omega_i$ , the state  $|0\rangle$  is the optimal state. Without the adaptive control, however, this state is only optimal at the beginning of the evolution. It will evolve away from this optimal point. The adaptive control, on the other hand, can keep the state at the optimal point and thus achieves the highest precision for all parameters simultaneously.

## VII. CONCLUSION

We have explicitly obtained the optimal probe states and measurements for the joint estimation of multiple Rabi frequencies and compared with the separate estimation. These results show that without adaptive controls there exist some time points at which the two Rabi frequencies in a three-level system cannot be jointly estimated. There also exist different regimes where the joint estimation can either outper-

form or underperform the separate estimation. However, with additional adaptive controls, the joint estimation can always outperform the separate estimation. This adds concrete results to the literature on the optimal performance of multiparameter quantum estimation.

## ACKNOWLEDGMENTS

The work is partially supported by the Research Grants Council of Hong Kong (GRF No. 14207717) and a direct Grant of CUHK (Grant No. 4055078).

## APPENDIX: OPTIMAL PROBE STATE FOR THE JOINT ESTIMATION OF TWO RABI FREQUENCIES

We write the pure input state in the eigenbasis of the Hamiltonian  $H$  as  $|\psi_{\text{in}}\rangle = C_0|\Phi_0\rangle + C_+|\Phi_+\rangle + C_-|\Phi_-\rangle$ , where  $C_0 \in \mathbb{R}$  and  $C_{\pm} \in \mathbb{C}$  are coefficients to be optimized. The evolution of the input state is described by the unitary operator  $U = e^{-iH(\Omega)t}$ . Therefore the output state is

$$|\psi_{\Omega}\rangle = e^{-iH(\Omega)t}|\psi_{\text{in}}\rangle = \left( \sum_{n=0,\pm} e^{-i\Omega_n t} |\Phi_n\rangle \langle \Phi_n| \right) |\psi_{\text{in}}\rangle. \quad (\text{A1})$$

The partial derivative of the state with respect to the  $i$ th parameter  $\Omega_i$  is given by

$$|\partial_i \psi_{\Omega}\rangle = \left( \sum_{n=0,\pm} \partial(e^{-i\Omega_n t} |\Phi_n\rangle \langle \Phi_n|) / \partial \Omega_i \right) |\psi_{\text{in}}\rangle = \sum_{n=0,\pm} (\langle \partial_i \Phi_n | \psi_{\text{in}} \rangle - it C_n \partial_i \Omega_n) e^{-i\Omega_n t} |\Phi_n\rangle + C_n e^{-i\Omega_n t} |\partial_i \Phi_n\rangle. \quad (\text{A2})$$

Note that

$$|\partial_i \Phi_0\rangle = -\frac{1}{\sqrt{2}} (\partial_i \vartheta) (|\Phi_+\rangle + |\Phi_-\rangle), \quad |\partial_i \Phi_{\pm}\rangle = \frac{1}{\sqrt{2}} (\partial_i \vartheta) |\Phi_0\rangle, \quad (\text{A3})$$

hence

$$\langle \partial_i \Phi_0 | \psi_{\text{in}} \rangle = -\frac{1}{\sqrt{2}} (\partial_i \vartheta) (C_+ + C_-), \quad \langle \partial_i \Phi_{\pm} | \psi_{\text{in}} \rangle = \frac{1}{\sqrt{2}} (\partial_i \vartheta) C_0. \quad (\text{A4})$$

Substituting Eq. (A4) in Eq. (A2), we can get the explicit form of  $|\partial_i \psi_{\Omega}\rangle$  expanded by the eigenbasis of  $H$ :

$$\begin{aligned} |\partial_i \psi_{\Omega}\rangle &= \frac{1}{\sqrt{2}} (\partial_i \vartheta) [C_+(e^{-i\Omega_+ t} - 1) + C_-(e^{-i\Omega_- t} - 1)] |\Phi_0\rangle + \left[ -it C_+(\partial_i \Omega_+) e^{-i\Omega_+ t} + \frac{1}{\sqrt{2}} C_0 (\partial_i \vartheta) (e^{-i\Omega_+ t} - 1) \right] |\Phi_+\rangle \\ &\quad + \left[ -it C_-(\partial_i \Omega_-) e^{-i\Omega_- t} + \frac{1}{\sqrt{2}} C_0 (\partial_i \vartheta) (e^{-i\Omega_- t} - 1) \right] |\Phi_-\rangle, \end{aligned} \quad (\text{A5})$$

where  $i = 1$  or  $2$ , and

$$\partial_1 \vartheta = \frac{\partial \vartheta}{\partial \Omega_1} = \frac{\Omega_2}{4\Omega_+^2}, \quad \partial_2 \vartheta = \frac{\partial \vartheta}{\partial \Omega_2} = -\frac{\Omega_1}{4\Omega_+^2}, \quad \partial_1 \Omega_+ = \frac{\partial \Omega_+}{\partial \Omega_1} = \frac{\Omega_1}{4\Omega_+}, \quad \partial_2 \Omega_+ = \frac{\partial \Omega_+}{\partial \Omega_2} = \frac{\Omega_2}{4\Omega_+}. \quad (\text{A6})$$

Recall that the SLD operators for the pure state  $|\psi_{\Omega}\rangle$  can be calculated by  $L_i = 2(|\partial_i \psi_{\Omega}\rangle \langle \psi_{\Omega}| + |\psi_{\Omega}\rangle \langle \partial_i \psi_{\Omega}|)$ ,  $i = 1$  or  $2$ . Thus the entries of the SLD Fisher information matrix can be calculated by

$$[J_{\Omega}]_{ij} = \frac{1}{2} \text{Tr}(|\psi_{\Omega}\rangle \langle \psi_{\Omega}| \{L_i, L_j\}) = 2(\langle \partial_i \psi_{\Omega} | \partial_j \psi_{\Omega} \rangle + \langle \partial_j \psi_{\Omega} | \partial_i \psi_{\Omega} \rangle) + 4 \langle \partial_i \psi_{\Omega} | \psi_{\Omega} \rangle \langle \partial_j \psi_{\Omega} | \psi_{\Omega} \rangle. \quad (\text{A7})$$

Denote  $P = e^{-i\Omega_+ t} - 1$ ,  $M = C_+^* P^* + C_-^* P$ , and  $N = C_+^* P^* - C_-^* P$ . First we consider when  $P = 0$ . In this case,

$$\langle \partial_i \psi_{\Omega} | \psi_{\Omega} \rangle = it (\partial_i \Omega_+) (|C_+|^2 - |C_-|^2), \quad (\text{A8})$$

$$\langle \partial_i \psi_{\Omega} | \partial_j \psi_{\Omega} \rangle = (\partial_i \Omega_+) (\partial_j \Omega_+) t^2 (1 - C_0^2). \quad (\text{A9})$$

Substituting them in Eq. (A7), we can get the QFIM as

$$J_{\Omega} = 4t^2 [1 - C_0^2 - (|C_+|^2 - |C_-|^2)^2] \begin{pmatrix} (\partial_1 \Omega_+)^2 & (\partial_1 \Omega_+) (\partial_2 \Omega_+) \\ (\partial_2 \Omega_+) (\partial_1 \Omega_+) & (\partial_2 \Omega_+)^2 \end{pmatrix}. \quad (\text{A10})$$

It can be easily seen that the QFIM is singular, indicating that we cannot estimate  $\Omega_1$  and  $\Omega_2$  simultaneously.

When  $P \neq 0$ , we have

$$\langle \partial_i \psi_{\Omega} | \psi_{\Omega} \rangle = i\sqrt{2} (\partial_i \vartheta) C_0 \text{Im}[(C_+^* P^* + C_-^* P)] + it (\partial_i \Omega_+) (|C_+|^2 - |C_-|^2) = i\sqrt{2} (\partial_i \vartheta) C_0 \text{Im}M + it (\partial_i \Omega_+) \frac{\text{Re}(MN^*)}{|P|^2} \quad (\text{A11})$$

and

$$\begin{aligned}
\langle \partial_i \psi_\Omega | \partial_j \psi_\Omega \rangle &= (\partial_i \Omega_+) (\partial_j \Omega_+) t^2 + [(\partial_i \vartheta) (\partial_j \vartheta) |P|^2 - (\partial_i \Omega_+) (\partial_j \Omega_+) t^2] C_0^2 + \frac{1}{2} (\partial_i \vartheta) (\partial_j \vartheta) |C_+^* P^* + C_-^* P|^2 \\
&\quad + i \frac{1}{\sqrt{2}} (\partial_i \Omega_+) (\partial_j \vartheta) t C_0 (C_-^* P - C_+^* P^*) + i \frac{1}{\sqrt{2}} (\partial_j \Omega_+) (\partial_i \vartheta) t C_0 (C_+ P - C_- P^*) \\
&= (\partial_i \Omega_+) (\partial_j \Omega_+) t^2 + [(\partial_i \vartheta) (\partial_j \vartheta) |P|^2 - (\partial_i \Omega_+) (\partial_j \Omega_+) t^2] C_0^2 + \frac{1}{2} (\partial_i \vartheta) (\partial_j \vartheta) |M|^2 + i \frac{-1}{\sqrt{2}} (\partial_i \Omega_+) (\partial_j \vartheta) t C_0 N \\
&\quad + i \frac{1}{\sqrt{2}} (\partial_j \Omega_+) (\partial_i \vartheta) t C_0 N^*, \tag{A12}
\end{aligned}$$

where  $\text{Re}(x)$  and  $\text{Im}(x)$  denote the real and imaginary parts of  $x$ , respectively. Substituting Eqs. (A11) and (A12) in Eq. (A7), we can get

$$\begin{aligned}
[J_\Omega]_{ij} &= 2(\langle \partial_i \psi_\Omega | \partial_j \psi_\Omega \rangle + \langle \partial_j \psi_\Omega | \partial_i \psi_\Omega \rangle) + 4 \langle \partial_i \psi_\Omega | \psi_\Omega \rangle \langle \partial_j \psi_\Omega | \psi_\Omega \rangle \\
&= (\partial_i \vartheta) (\partial_j \vartheta) (-8C_0^2 \text{Im}^2 M + 4C_0^2 |P|^2 + 2|M|^2) + (\partial_i \Omega_+) (\partial_j \Omega_+) \left( -4t^2 \frac{\text{Re}^2(MN^*)}{|P|^4} + 4t^2 - 4C_0^2 t^2 \right) \\
&\quad + [(\partial_i \vartheta) (\partial_j \Omega_+) + (\partial_j \vartheta) (\partial_i \Omega_+)] \left( -4\sqrt{2}C_0 \text{Im} M \frac{\text{Re}(MN^*)}{|P|^2} t + 2\sqrt{2}C_0 t \text{Im} N \right) \\
&= (\partial_i \vartheta) (\partial_j \vartheta) A + (\partial_i \Omega_+) (\partial_j \Omega_+) B + [(\partial_i \vartheta) (\partial_j \Omega_+) + (\partial_j \vartheta) (\partial_i \Omega_+)] C, \tag{A13}
\end{aligned}$$

where  $A = -8C_0^2 \text{Im}^2 M + 4C_0^2 |P|^2 + 2|M|^2$ ,  $B = -4t^2 \frac{\text{Re}^2(MN^*)}{|P|^4} + 4t^2 - 4C_0^2 t^2$ , and  $C = -4\sqrt{2}C_0 \text{Im} M \frac{\text{Re}(MN^*)}{|P|^2} t + 2\sqrt{2}C_0 t \text{Im} N$ . It then straightforward to get

$$\begin{aligned}
\text{Tr}(J_\Omega^{-1}) &= \frac{[(\partial_P \vartheta) (\partial_P \vartheta) + (\partial_S \vartheta) (\partial_S \vartheta)] A + 2[(\partial_P \vartheta) (\partial_P \Omega_+) + (\partial_S \vartheta) (\partial_S \Omega_+)] C + [(\partial_P \Omega_+) (\partial_P \Omega_+) + (\partial_S \Omega_+) (\partial_S \Omega_+)] B}{[(\partial_P \vartheta) (\partial_S \Omega_+) - (\partial_S \vartheta) (\partial_P \Omega_+)]^2 (AB - C^2)} \\
&= \frac{(1/4\Omega_+^2) A + (1/4) B}{(1/16\Omega_+^2)(AB - C^2)} = \frac{4A + 4\Omega_+^2 B}{AB - C^2}. \tag{A14}
\end{aligned}$$

Since  $|M|^2 + |N|^2 = 2|P|^2(1 - C_0^2)$ , we can let

$$M = \sqrt{2|P|^2(1 - C_0^2)} e^{i\alpha} \cos \theta, \quad N = \sqrt{2|P|^2(1 - C_0^2)} e^{i\beta} \sin \theta. \tag{A15}$$

Then

$$\begin{aligned}
A &= 4|P|^2 C_0^2 + 4|P|^2 (1 - C_0^2) \cos^2 \theta - 16|P|^2 C_0^2 (1 - C_0^2) \cos^2 \theta \sin^2 \alpha, \\
B &= 4t^2 (1 - C_0^2) - 4t^2 (1 - C_0^2)^2 \sin^2 2\theta \cos^2(\alpha - \beta). \tag{A16}
\end{aligned}$$

With this we are going to show that  $\frac{A}{AB - C^2} \geq \frac{1}{4t^2}$  and  $\frac{B}{AB - C^2} \geq \frac{1}{4|P|^2}$ .

To show  $\frac{A}{AB - C^2} \geq \frac{1}{4t^2}$ , we note that

$$\frac{A}{AB - C^2} - \frac{1}{4t^2} = \frac{4t^2 A - (AB - C^2)}{4t^2 (AB - C^2)} \geq \frac{A(4t^2 - B)}{4t^2 (AB - C^2)}. \tag{A17}$$

From the fact that the quantum Fisher information matrix is positive semidefinite, we can obtain  $AB - C^2 \geq 0$ . Also

$$\begin{aligned}
A &\geq 4|P|^2 C_0^2 \cos^2 \theta + 4|P|^2 (1 - C_0^2) \cos^2 \theta - 16|P|^2 C_0^2 (1 - C_0^2) \cos^2 \theta \sin^2 \alpha \\
&\geq 4|P|^2 \cos^2 \theta - 4|P|^2 \cos^2 \theta \sin^2 \alpha \geq 0, \tag{A18}
\end{aligned}$$

where we used the fact  $4C_0^2(1 - C_0^2) \leq 1$  and

$$4t^2 - B = 4t^2 C_0^2 + 4t^2 (1 - C_0^2)^2 \sin^2 2\theta \cos^2(\alpha - \beta) \geq 0. \tag{A19}$$

Thus  $\frac{A}{AB - C^2} - \frac{1}{4t^2} \geq 0$ . The equality can be saturated when  $C = 0$  and  $B = 4t^2$ .

To show  $\frac{B}{AB - C^2} \geq \frac{1}{4|P|^2}$ , we note that

$$\frac{B}{AB - C^2} - \frac{1}{4|P|^2} = \frac{4|P|^2 B - (AB - C^2)}{4|P|^2 (AB - C^2)} \geq \frac{B(4|P|^2 - A)}{4|P|^2 (AB - C^2)}, \tag{A20}$$

since

$$B \geq 4t^2(1 - C_0^2) - 4t^2(1 - C_0^2)^2 = 4t^2C_0^2(1 - C_0^2) \geq 0 \quad (\text{A21})$$

and

$$4|P|^2 - A = 4|P|^2(1 - C_0^2)(1 - \cos^2 \theta) + 16|P|^2C_0^2(1 - C_0^2)\cos^2 \theta \sin^2 \alpha \geq 0. \quad (\text{A22})$$

Thus  $\frac{B}{AB-C^2} - \frac{1}{4|P|^2} \geq 0$  and the equality can be saturated when  $C = 0$  and  $A = 4|P|^2$ .

With  $\frac{A}{AB-C^2} \geq \frac{1}{4t^2}$  and  $\frac{B}{AB-C^2} \geq \frac{1}{4|P|^2}$ , it is then easy to see that

$$\text{Tr}(J_\Omega^{-1}) = \frac{4A + 4\Omega_+^2 B}{AB - C^2} \geq \frac{1}{t^2} + \frac{\Omega_+^2}{|P|^2} = \frac{1}{t^2} + \frac{\Omega_+^2}{4 \sin^2(\Omega_+ t/2)}, \quad (\text{A23})$$

where the equality can be achieved with  $A = 4|P|^2$ ,  $B = 4t^2$ , and  $C = 0$ . It is straightforward to check that when the input state takes the form  $|\psi_{\text{in}}\rangle = P^*/(\sqrt{2}|P|)|\Phi_+\rangle + P/(\sqrt{2}|P|)|\Phi_-\rangle$ , the equality is saturated, and thus it is the optimal probe state. Since  $P = e^{-i\Omega_+ t} - 1 = -2i \sin(\Omega_+ t/2)e^{-i\Omega_+ t/2}$ , the optimal input state can also be written as

$$|\psi_{\text{in}}\rangle = \frac{P^*}{\sqrt{2}|P|}|\Phi_+\rangle + \frac{P}{\sqrt{2}|P|}|\Phi_-\rangle = \frac{e^{i\Omega_+ t/2}|\Phi_+\rangle - e^{i\Omega_- t/2}|\Phi_-\rangle}{\sqrt{2}}. \quad (\text{A24})$$

- 
- [1] C. L. Degen, F. Reinhard, and P. Cappellaro, *Rev. Mod. Phys.* **89**, 035002 (2017).
  - [2] D. Braun, G. Adesso, F. Benatti, R. Floreanini, U. Marzolino, M. W. Mitchell, and S. Pirandola, *Rev. Mod. Phys.* **90**, 035006 (2018).
  - [3] C. F. Roos, M. Chwalla, K. Kim, M. Riebe, and R. Blatt, *Nature (London)* **443**, 316 (2006).
  - [4] I. D. Leroux, M. H. Schleier-Smith, and V. Vuletić, *Phys. Rev. Lett.* **104**, 073602 (2010).
  - [5] A. Louchet-Chauvet, J. Appel, J. J. Renema, D. Oblak, N. Kjaergaard, and E. S. Polzik, *New J. Phys.* **12**, 065032 (2010).
  - [6] O. Hosten, N. J. Engelsen, R. Krishnakumar, and M. A. Kasevich, *Nature (London)* **529**, 505 (2016).
  - [7] L. Pezzè, A. Smerzi, M. K. Oberthaler, R. Schmied, and P. Treutlein, *Rev. Mod. Phys.* **90**, 035005 (2018).
  - [8] D. Leibfried, *Science* **304**, 1476 (2004).
  - [9] P. O. Schmidt, *Science* **309**, 749 (2005).
  - [10] E. Davis, G. Bentsen, and M. Schleier-Smith, *Phys. Rev. Lett.* **116**, 053601 (2016).
  - [11] R. Shani, T. Manovitz, Y. Shapira, N. Akerman, and R. Ozeri, *Phys. Rev. Lett.* **120**, 243603 (2018).
  - [12] M. Koschorreck, M. Napolitano, B. Dubost, and M. W. Mitchell, *Phys. Rev. Lett.* **104**, 093602 (2010).
  - [13] R. J. Sewell, M. Koschorreck, M. Napolitano, B. Dubost, N. Behbood, and M. W. Mitchell, *Phys. Rev. Lett.* **109**, 253605 (2012).
  - [14] J. B. Brask, R. Chaves, and J. Kołodyński, *Phys. Rev. X* **5**, 031010 (2015).
  - [15] S. Schmitt, T. Gefen, F. M. Stürner, T. Unden, G. Wolff, C. Müller, J. Scheuer, B. Naydenov, M. Markham, S. Pezzagna, J. Meijer, I. Schwarz, M. Plenio, A. Retzker, L. P. McGuinness, and F. Jelezko, *Science* **356**, 832 (2017).
  - [16] R. Schnabel, N. Mavalvala, D. E. McClelland, and P. K. Lam, *Nat. Commun.* **1**, 121 (2010).
  - [17] LIGO Scientific Collaboration, *Nat. Photonics* **7**, 613 (2013).
  - [18] R. X. Adhikari, *Rev. Mod. Phys.* **86**, 121 (2014).
  - [19] B. P. Abbott *et al.* (LIGO Scientific Collaboration and Virgo Collaboration), *Phys. Rev. Lett.* **116**, 061102 (2016).
  - [20] V. Giovannetti, *Science* **306**, 1330 (2004).
  - [21] V. Giovannetti, S. Lloyd, and L. Maccone, *Phys. Rev. Lett.* **96**, 010401 (2006).
  - [22] V. Giovannetti, S. Lloyd, and L. Maccone, *Nat. Photonics* **5**, 222 (2011).
  - [23] C. Preza, D. L. Snyder, and J.-A. Conchello, *J. Opt. Soc. Am. A* **16**, 2185 (1999).
  - [24] G. Brida, M. Genovese, and I. Ruo Berchera, *Nat. Photonics* **4**, 227 (2010).
  - [25] G. H. Low, T. J. Yoder, and I. L. Chuang, *Phys. Rev. Lett.* **114**, 100801 (2015).
  - [26] C. Lupo and S. Pirandola, *Phys. Rev. Lett.* **117**, 190802 (2016).
  - [27] R. Nair and M. Tsang, *Phys. Rev. Lett.* **117**, 190801 (2016).
  - [28] R. McConnell, G. H. Low, T. J. Yoder, C. D. Bruzewicz, I. L. Chuang, J. Chiaverini, and J. M. Sage, *Phys. Rev. A* **96**, 051801 (2017).
  - [29] R. Nair, *Phys. Rev. Lett.* **121**, 230801 (2018).
  - [30] P. C. Humphreys, M. Barbieri, A. Datta, and I. A. Walmsley, *Phys. Rev. Lett.* **111**, 070403 (2013).
  - [31] T. Baumgratz and A. Datta, *Phys. Rev. Lett.* **116**, 030801 (2016).
  - [32] R. D. Gill and S. Massar, *Phys. Rev. A* **61**, 042312 (2000).
  - [33] N. Li, C. Ferrie, J. A. Gross, A. Kalev, and C. M. Caves, *Phys. Rev. Lett.* **116**, 180402 (2016).
  - [34] A. Acín, E. Jané, and G. Vidal, *Phys. Rev. A* **64**, 050302 (2001).
  - [35] A. Fujiwara, *Phys. Rev. A* **65**, 012316 (2001).
  - [36] M. A. Ballester, *Phys. Rev. A* **69**, 022303 (2004).
  - [37] S. D. Bartlett, T. Rudolph, and R. W. Spekkens, *Rev. Mod. Phys.* **79**, 555 (2007).
  - [38] J. Liu, X.-X. Jing, and X. Wang, *Sci. Rep.* **5**, 8565 (2015).
  - [39] X.-Q. Zhou, H. Cable, R. Whittaker, P. Shadbolt, J. L. O'Brien, and J. C. F. Matthews, *Optica* **2**, 510 (2015).

- [40] D. W. Berry, M. Tsang, M. J. W. Hall, and H. M. Wiseman, *Phys. Rev. X* **5**, 031018 (2015).
- [41] M. D. Vidrighin, G. Donati, M. G. Genoni, X.-M. Jin, W. S. Kolthammer, M. Kim, A. Datta, M. Barbieri, and I. A. Walmsley, *Nat. Commun.* **5**, 3532 (2014).
- [42] P. J. D. Crowley, A. Datta, M. Barbieri, and I. A. Walmsley, *Phys. Rev. A* **89**, 023845 (2014).
- [43] A. Monras and F. Illuminati, *Phys. Rev. A* **83**, 012315 (2011).
- [44] Y. Chen and H. Yuan, *New J. Phys.* **19**, 063023 (2017).
- [45] L. Pezzè, M. A. Ciampini, N. Spagnolo, P. C. Humphreys, A. Datta, I. A. Walmsley, M. Barbieri, F. Sciarrino, and A. Smerzi, *Phys. Rev. Lett.* **119**, 130504 (2017).
- [46] Y. Yang, G. Chiribella, and M. Hayashi, arXiv:1802.07587.
- [47] H. Yuan and C.-H. F. Fung, *Phys. Rev. A* **96**, 012310 (2017).
- [48] H. Yuan and C.-H. F. Fung, *npj Quantum Inf.* **3**, 14 (2017).
- [49] H. Yuan and C.-H. F. Fung, *New J. Phys.* **19**, 113039 (2017).
- [50] H. Yuan, *Phys. Rev. Lett.* **117**, 160801 (2016).
- [51] R. A. Fisher, *Math. Proc. Cambridge Philos. Soc.* **22**, 700 (1925).
- [52] H. Cramér, *Mathematical Methods of Statistics* (Princeton University, Princeton, NJ, 1946), p. 591.
- [53] C. R. Rao, *Breakthroughs in Statistics: Foundations and Basic Theory* 37, 81 (Springer, New York, 1992), pp. 235–247.
- [54] S. M. Kay, *Fundamentals of Statistical Signal Processing: Estimation Theory* (Prentice-Hall, New York, 1993).
- [55] C. W. Helstrom, *Quantum Detection and Estimation Theory*, Mathematics in Science and Engineering (Academic, New York, 1976), Vol. 123.
- [56] A. S. Holevo, *Probabilistic and Statistical Aspects of Quantum Theory* (Springer, New York, 2011).
- [57] S. L. Braunstein and C. M. Caves, *Phys. Rev. Lett.* **72**, 3439 (1994).
- [58] K. Matsumoto, *J. Phys. A: Math. Gen.* **35**, 3111 (2002).
- [59] S. Ragy, M. Jarzyna, and R. Demkowicz-Dobrzański, *Phys. Rev. A* **94**, 052108 (2016).
- [60] J. Yang, S. Pang, Y. Zhou, and A. N. Jordan, arXiv:1806.07337.
- [61] H. Yuan and C.-H. F. Fung, *Phys. Rev. Lett.* **115**, 110401 (2015).
- [62] J. Liu and H. Yuan, *Phys. Rev. A* **96**, 012117 (2017).
- [63] J. Liu and H. Yuan, *Phys. Rev. A* **96**, 042114 (2017).
- [64] S. Pang and A. N. Jordan, *Nat. Commun.* **8**, 14695 (2017).